Structure and Properties of DNA-Based Reversible Polymers

Jun Xu, Elizabeth A. Fogleman, and Stephen L. Craig*

Department of Chemistry and Center for Biologically Inspired Materials and Materials Systems, Duke University, Durham, North Carolina 27708-0346

Received October 14, 2003; Revised Manuscript Received December 15, 2003

ABSTRACT: Duplex formation between DNA-based monomers creates linear, polymeric assemblies that resemble larger duplex DNA, but in which the main chain is defined by the reversible base pairing. These monomers provide a reversible polymer platform through which molecule-to-material relationships can be explored. Viscometry, static and dynamic light scattering, and size exclusion chromatography are used to probe the size, structure, and dynamics of the systems. The influence of concentration, temperature, association constant, and conformational flexibility is examined and found to be consistent with simple equilibrium models. The characterizations provide the basis for further mechanistic studies of reversible polymeric behavior in complex environments.

Introduction

Linear polymers that are reversibly formed along their main chain (Figure 1) have gathered increasing attention in recent years.[1−12] These reversible polymers (RP's) consist of molecular building blocks that comprise two or more molecular recognition end groups that are covalently linked. At equilibrium, reversible association of the end groups defines the main chain of linear polymers.[5−12] The structure and properties of an RP depend on the strength and specificity of the association, the conformational flexibility of the molecule, the concentration of the monomer, and the chemical and physical environment of the system. RP's are dissipative, and they undergo conformational changes and diffusion on much shorter time scales than their covalent counterparts and assemble with minimal imperfections. They offer promise as environmentally benign materials due to the ease of processing and recycling and the absence of a polymerization catalyst. RP's are furthermore unique relative to their covalent analogues in that fracture at the reversible junctions along the main chain can be repaired because end-group dissociation and reassociation is a dynamic, equilibrium process.[7,13] Reported RP's encompass a range of structural motifs, phase behaviors,[7,9,11,14−16] solution and solid-state mechanical properties,[8,17,18] and environmental responsiveness.[18]

Largely due to the above reasons, there is growing interest in RP's. Following the pioneering work of Lehn,[7] the past 12 years have seen increasing attention given to these materials. Griffin has used main-chain hydrogen bonding to create liquid crystalline RP's.[11] Stadler performed the first rheological characterization of main-chain hydrogen-bonded polymer properties.[19] Meijer increased the association constant and achieved high molecular weights through a quadruple hydrogen-bonded motif.[8,15,20−23] His group showed for the first time that reversible polymers may possess properties that are similar to traditional covalent polymers despite the transient interaction (lifetime on the order of seconds) defining the main chain. Castellano and Rebek have combined main-chain hydrogen bonding with guest encapsulation, creating polymeric assemblies with new types of chemical responsiveness.[9] Rehahn is credited with the first soluble RP's based on metal−ligand interactions,[24] and Schubert has recently reported a series of RP's that are defined by metal−ligand coordination.[25−34] Generally, increasing numbers of supramolecular approaches to material science are being explored.[3,35−49] These discoveries illustrate that the potential environmental and mechanical properties of RP's might be broadly applied to a range of materials applications, if the underlying molecular mechanisms of their properties were fully understood and exploited.

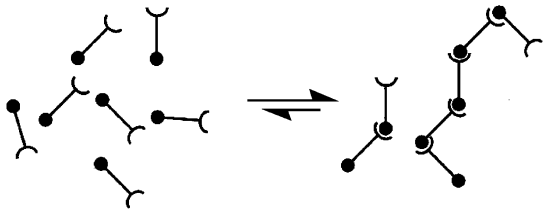

Figure 1. Schematic of the formation of linear, reversible polymers. The ball and bracket represent two complementary recognition end groups that are covalently linked.

While RP's have the potential to last longer and be more environmentally friendly than conventional, covalent polymers, several design criteria must be balanced before they can be used for commercial applications. For example, if the reversible association is too weak, the resulting polymer molecular weight will be low and mechanical properties will suffer. Conversely, if the association is too strong, the time scale for dissociation eventually becomes too slow to permit the reequilibration that engenders responsiveness. Studies on individual systems, in particular those done by Meijer and his group,[8,50,51] show that a useful middle ground exists. RP's developed by Meijer and others exhibit physical properties that are truly "polymeric", such as modulus, shear-thinning, and substantial normal forces, and well-ordered RP fibers possess tensile strengths that approach those of commercial nylon fibers while still being recyclable through simple methanol titration.[18]

* Corresponding author: e-mail stephen.craig@duke.edu.

10.1021/ma035546v CCC: $27.50
Published on Web 01/29/2004

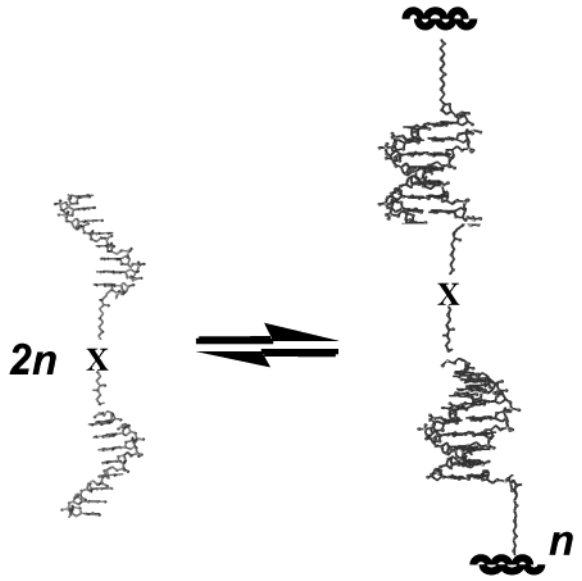

Figure 2. DNA-based modular system. Two independent oligonucleotides (left side) are linked either directly (when X is null) or through coupling to a synthetic spacer unit (when $X = -CH_2CH_2CH_2-$ or $-(CH_2CH_2O)_6-$). $2n$ and n represent the number of monomers on the left and the number of repeating units on the right, respectively.

An ongoing challenge for chemists is to relate behavior at the level of polymer physics to behavior at the molecular level. For example, what are the ideal association constant and the ideal kinetics for equilibration or the necessary number of reversible interactions? Or more generally, what is the quantitative relationship between the thermodynamics and kinetics of the reversible association, the structure of the monomer, and the structure and properties of the reversible polymer? The answer to these questions, of course, likely depends on the specifics of the system and the desired application. Nevertheless, if general relationships were established, materials properties could be controlled in a rational way through small-molecule synthesis.

To that end, we recently reported that reversible polymers formed from oligonucleotide-based monomers (hereafter OM's) are a useful model system for delineating molecule-to-material relationships in RP's.[52] The OM's comprise oligonucleotide sequences that are covalently linked directly or through a synthetic spacer (Figure 2). Duplex formation creates a linear, polymeric assembly that resembles larger duplex DNA, but in which the main chain is defined by the reversible base pairing. Recent work by Rowan[36] also makes use of nucleobases to engender polymeric properties, although the system, and possibly mechanism, differs dramatically from the approach reported here. The RP's formed from OM's are intrinsically modular, and they are therefore amenable to "physical organic chemistry of materials"—systematically varying the structure of the components and observing concomitant changes in the properties of the assemblies.

This utility of the DNA-based modules results from the wide range of structural variations permitted in the monomers (Table 1). The thermodynamics and kinetics of the association are determined by the variable base sequence. The linear density of the reversible interactions, and the conformational flexibility along the polymer backbone, are each dependent on a spacer in which much variation is possible. Inter- and intrachain interactions may be tuned by salt concentration in the buffer. Robust enzymology offers covalent capture of transient structures and structural analyses of cyclizations, and the systems are true or only moderately perturbed analogues of well-studied DNA duplexes of similar molecular weight.[52,53]

Table 1. Structural Handles in Oligonucleotide-Based Reversible Polymers

desired element of control	OM handle
association thermodynamics	base sequences
association dynamics	base sequences
polymer conformation	spacer flexibility
no. of reversible associations	spacer length
polymer−polymer interactions	buffer concentration
covalent capture	enzymatic ligation

The latter trait places clear limits on the practical utility of OM's. The cost of synthesis precludes production of bulk materials. The polyelectrolyte nature of the polymers and short-range repulsion between chains are inherent features of the system. Solubility restricts solution studies to semidilute concentrations of less than ca. 50 mg mL^{-1}. There remains, however, rich polymer physics within these boundaries, and the modularity of the system allows for a thorough exploration of that terrain.

Among the physics of greatest interest is that found in spatially constrained environments, for example between surfaces and at interfaces. The spatial constraints impose on large macromolecules steric interactions on the order of kT per polymer chain, and unlike conventional polymers, RP's can adjust their local size in response to these steric interactions. Because an energy difference of kT in chemical potential corresponds to a change of ~40% in RP molecular weight, the structural differences and concomitant properties of RP's relative to conventional polymers might be dramatic. Further interest is in the dynamic behavior of interfacial RP's away from equilibrium, for example under dynamic mechanical stress or in a concentration gradient. In these nonequilibrium environments, main-chain dynamics might contribute to RP dynamic properties and engender responsiveness not found in covalent systems.

The polymer physics in such environments is necessarily complex, and the modularity of the OM's is well-suited to fundamental studies in these areas. A firm understanding of OM-based RP equilibrium structure is required, however, to approach these more complex problems properly. Here we extend our initial study and report further details of OM-based equilibrium RP structure and properties. Viscometry, static, and dynamic light scattering and size exclusion chromatography are used to probe the size, structure, and dynamics of the systems in response to changes in concentration, temperature, OM structure, and association constant. The onset of chain overlap in the semidilute concentration regime is also established. The theory of equilibrium RP structure in dilute solutions is well-established, and the characterizations reported here verify that the behavior of the OM's is consistent with those equilibrium models. The studies, however, also reveal unanticipated yet significant thermodynamic, structural, and dynamic effects in these OM-based systems. On the whole, this work confirms the utility of OM's as a modular RP platform, and it provides the basis for ongoing mechanistic studies of more complex RP behavior, for example at surfaces and interfaces.[6]

Table 2. Composition and Experimentally Determined Free Energies of Association of Oligonucleotides from UV Melting Studies

OM	sequence (from **5′→3′**)	ΔG_{UV}(298 K) (kcal/mol)
1	CGTATACGGCCTAGGC	−12.2
2	GGTATACCGCTTAAGC	−10.3
3	GGTATACCGTTTAAAC	−9.4
4	GGTATACC−$(CH_2CH_2O)_6$−GCTTAAGC	−8.8
5	GGTATACC−$CH_2CH_2CH_2$−GCTTAAGC	−8.3
6	GGTATACCGC	

Experimental Methods

Materials. Oligonucleotides **1**−**3** and **6** were synthesized by DNAgency, using commercial synthesizers and standard phosphoramidite synthesis procedures. To synthesize the oligonucleotides **4** and **5**, 3-(4,4′-dimethoxytrityloxy)propyl-1-[(2-cyanoethyl)−(*N*,*N*-diisopropyl)]phosphoramidite and 18-*O*-dimethoxytritylhexaethylene glycol,1-[(2-cyanoethyl)-(*N*,*N*-diisopropyl)]phosphoramidite (Glen Research) were incorporated following the manufacturer's instructions by the Duke University DNA Core Facility using standard phosphoramidite coupling procedures. All monomers were received trityl-on and subsequently purified and deprotected in-house using a Varian RP HPLC and Dynamax pure DNA column. Oligonucleotides were dissolved in a 1 M NaCl and 10 mM sodium phosphate buffer at pH 7.2. Subsequent HPLC analysis of the oligonucleotides shows no evidence (<1%) for shorter oligonucleotide impurities from failure sequences.

Design of Oligonucleotide Monomers (OM). Representative oligonucleotides are listed in Table 2. A typical monomer consists of two 8-mer oligonucleotides in which the eight bases from 5′ to 3′ are self-complementary from 3′ to 5′. OM's **1**−**5** are self-complementary. OM **6** is designed as a chain terminator of **2**−**5**, and it consists of only one of the two 8-mer constituents of **2**−**5** with an additional two-base overhang to balance thermodynamics.[54,55] To maximize selectivity, sequences were designed so that no three-base overlaps were possible except within the desired eight-base duplexes.

Thermal melting measurements were performed according to literature procedures.[56a] Melting curves were measured at 260 nm in a standard rectangular far-UV quartz cuvette with a 10 mm path length and a Hewlett-Packard 845x UV−vis spectrophotometer. Curves were obtained at five different concentrations, typically from 8.5×10^{-7} to 1.3×10^{-5} M. As previously reported for the association of self-complementary OM's,[56b] $1/T_m = (R/\Delta H°) \ln(C_t) + \Delta S°/\Delta H°$ and $K_{eq}(T_m) = 1/C_t$, where T_m is the melting temperature at a total monomer concentration of C_t, R is the gas constant (8.314 J/(K mol)), and K_{eq}, $\Delta H°$, and $\Delta S°$ are the equilibrium constant, the standard enthalpy change, and entropy change in the process of thermal melting, respectively. Thermodynamic parameters are extracted from plots of $1/T_m$ vs $\ln(C_t)$.

Viscosity measurements were performed in a Cannon-Ubbelohde semi-microdilution type viscometer. Typically, ∼1 mL solution of monomer was pipetted into a viscometer whose temperature was maintained by a CT-500 Cannon constant temperature bath. Chain termination studies were performed by adding 1−10% (by weight vs OM) of chain terminator **6** from a stock solution. The actual volume added was determined by weighing the viscometer. Solutions were mixed well and annealed four times between 20 and 50 °C prior to viscosity measurements. Higher viscosities were measured on a Bohlin CVO rheometer, equipped with cone and plate geometry. At least three trials were repeated for each sample at each temperature, and the statistical uncertainty in the measurements was less than 1%.

Light scattering instrumentation comprised the Wyatt Technology DAWN EOS MALS detector with a 30 mW solid-state laser operating at 690 nm and the Wyatt Technology quasi-elastic light scattering detector with signals received from a Wyatt Technology fiber receiver positioned at 108° with respect to the direction of the laser beam. The refractive index increment (d*n*/d*c*) of the DNA solutions was 0.165 mL/g,[57] as confirmed by a Wyatt Optilab DSP interferometric refractometer. The OM samples were introduced in one of two ways: microcuvette or flow cell. In the microbatch experiments, the solutions were directly filtered into a microcuvette (Wyatt Technology), which is a rectangular cell made from fused spectrosil quartz, with 10 mm × 1 mm windows allowing scattered light to be measured at multiple angles from 66° to 110°. Sample solutions were filtered through a 0.01 μm filter (Protein-Solutions, Nanofilter systems) prior to use, and their concentrations were determined by UV absorbance after light scattering measurements. In the case of OM **4** and **5**, the sample was annealed by four heat/cool cycles between 20 and 50 °C. With the flow cell instead of the microcuvette, the concentration detector and light scattering detectors were connected to the eluting end of a Varian Prostar HPLC with an Agilent GF-250 size exclusion column. Weight-average molar mass (M_w), *z*-average root-mean-square (rms) radii of gyration, and hydrodynamic radii were obtained by standard calculations using ASTRA software (version 4.90.07 for Windows, Wyatt Technology Corp.).[58]

The second virial coefficient must be taken into account in the light scattering equation as a correction factor for concentration effects due to an increased intermolecular interference:

$$KC/R_{\theta=0} = 1/M_{app}(C) \approx 1/M_w + 2A_2C$$

where K is an optical constant related to the light wavelength, solvent refractive index, and refractive index increment. $R_{\theta=0}$ is the excess Rayleigh ratio at zero angle. We have determined that for the OM systems studied here in 1 M NaCl/10 mM NaH_2PO_4 buffer, $A_2 = 4.9 \times 10^{-4}$ mL mol/g^2,[59] a value that is somewhat higher than previous experimental determinations[60] but agrees very well with theoretical predictions.[57,61] The determination of A_2 allows us to measure accurate absolute molecular weights of the OM-based polymers.

Results and Discussion

A distinguishing feature of reversible polymers is the sensitivity of their primary structure to their environment.[1,3,8,18,51,62−64] At the most fundamental level, the molecular weight of a linear polymer reflects the relative percentages of bound (chain propagation) and unbound (chain termination) monomer end groups. At higher monomer concentrations C and association constants K_1 and K_2, the equilibrium between these two states shifts toward bound associations, and so the molecular weights of RP's, unlike those of covalent polymers, will increase as described in eq 1 (for a derivation, please see the Supporting Information).

$$DP = \frac{2C}{\dfrac{-1+\sqrt{1+8K_1C}}{4K_1} + \dfrac{-1+\sqrt{1+8K_2C}}{4K_2}} \quad (1)$$

where C is the concentration of monomer and K_1 and K_2 are the association constants of the two duplexes in the monomer.

Although all OM's used in this study have two different duplexes, only one melting transition was observed in thermal UV−vis studies. The experimental free energies of duplex formation, therefore, reflect an average value. In all cases, the experimental value is within 0.5 kcal mol^{-1} of the average of the empirically derived calculations for the two duplexes. We analyze our results in terms of this "effective" association constant K derived from the melting studies and employ a new eq 2 for purposes of discussion. If we assume the measured free energy is the average of those from two different parts, then the effective association constant

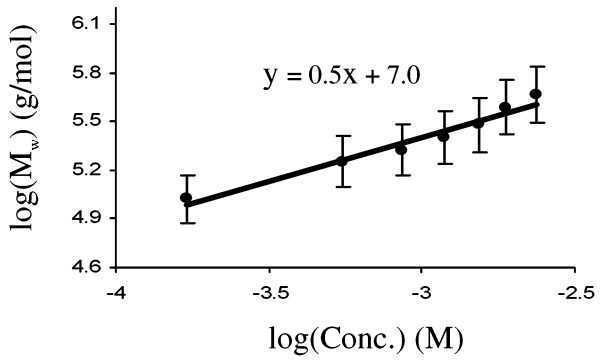

Figure 3. Concentration dependence of the weight-average molecular weights measured by light scattering (OM **2** at concentrations ranging from 0.16 to 2.30 mM). Error bars indicate the uncertainty in M_w as determined from the best fit to the Debye plots (ASTRA software, Wyatt).

K is the geometric mean of K_1 and K_2, and eq 2 can be obtained:

$$DP = \frac{4KC}{-1 + \sqrt{1 + 8KC}} \approx \sqrt{2KC} \qquad (2)$$

The error introduced by this assumption is small and does not influence the conclusions of this work. Using those same empirically derived relationships, the expected difference in association constants of the two duplexes in any OM is less than 1 order of magnitude. For the worst-case scenario, $K_1 = 10K_2$; the DP's (and hence polymer molecular weights) calculated by eqs 1 and 2 differ by <14%.

It should be noted that the molecular weight mentioned throughout this paper is the weight-average molecular weight of polydispersed aggregates, and it is represented as M_w hereafter. Experimental M_w's were directly measured from light scattering, whereas the theoretical M_w's were calculated by multiplying the number-average molecular weights based on the DP's from eq 2 with a theoretical polydispersity index (hereafter PDI) of PDI = 2 − (1/DP).

Concentration Dependence. As mentioned above, the molecular weight of RP's is sensitive to concentration because of the equilibrium between bound duplexes and free single strands. The expected effect of concentration on molecular weight is observed clearly for OM **2**. Polymer molecular weights, as determined by static multiangle light scattering (MALS) in microbatch mode, increase as **[2]**$^{0.5}$ (Figure 3), in excellent agreement with the square-root dependence expected from eq 1 or 2. The samples were prepared by sequential dilution of a single stock solution, and the change in M_w therefore is immediate evidence that the polymers are reversible.

Those reversible dynamics complicate other traditional methods of molecular weight characterization, for example size exclusion chromatography. When 100 μL of 0.54 mM OM **2** was injected into a size exclusion column coupled to a light scattering detector, the end result is shown in Figure 4. Some separation by molecular weight is achieved, with higher M_w polymers reaching the detector at earlier elution times. The average molecular weight of the sample, however, is 108 kDa, less than 182 kDa observed in the microbatch analysis of 0.54 mM OM **2**. Further, the polydispersity index (PDI) of the eluted polymer is 1.5, which is smaller than the value of 1.9 expected (corresponding to a DP of ∼10). These results suggest equilibration on the

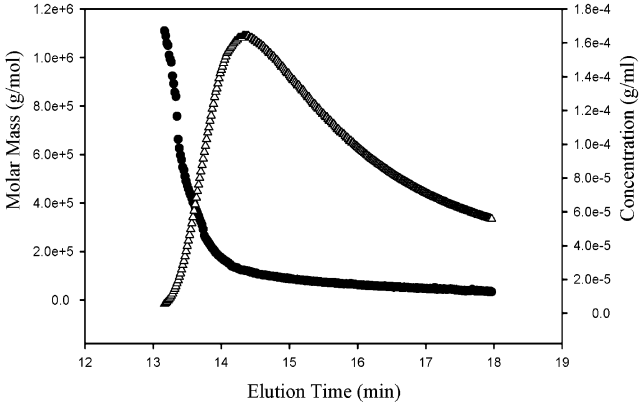

Figure 4. Separation of reversible polymers from OM **2** was achieved by size exclusion chromatography combined with light scattering detectors: (●) molar mass vs elution time; (△) concentration vs elution time.

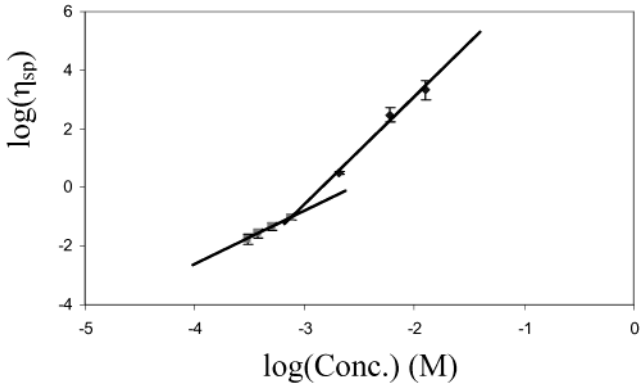

Figure 5. Concentration dependence of the specific viscosity of OM **2** solutions from 0.2 to 8 mM. The slope is 1.8 at dilute concentrations and 3.7 when the concentration is higher than ca. 0.8 mM. Error bars indicate the uncertainty in viscosities as determined from the standard deviation of at least three measurements.

column; as the OM is separated and diluted, equilibration of the diluted analyte lowers the average molecular weight.

On-column equilibration is verified by injecting different volumes of the same sample. The average molecular weight is higher for larger injection volumes. Because the samples are diluted into the same final mobile phase volume (as evidenced by the elution peak width), the ultimate relative concentration of OM is proportional to the injection volume. Polymer molecular weights of 108, 84, and 57 kDa are observed for injection volumes (V_{inj}) of 100, 50, and 25 μL, respectively. The M_w varies with $V_{inj}^{0.5}$, consistent with both the concentration dependence observed in the batch experiments and also that expected from theory.

Changes in concentration are also manifested in the viscosity of OM solutions. For OM **2**, solution viscosities initially vary with **[2]**$^{1.8}$, but for **[2]** > 0.8 mM (3.9 g/L) the dependence is **[2]**$^{3.7}$ (Figure 5).[65] The change in concentration dependence is indicative of a transition from the dilute to semidilute concentration regime, where overlap between chains contributes to viscous drag. The transition occurs at a concentration where the average volume per polymer molecule is approximately equal to the hydrodynamic volume of the polymer. Classically, the transition should occur at $C^* = 3M_w/(4\pi R_g^3 N_A)$, where N_A is Avogadro's number, and M_w and R_g are the molecular weight and the radius of gyration

Table 3. Relationship between Association Constants Measured by UV Melting Curves and Molecular Weights Measured by Light Scattering for OM 1−5 at the Concentration of 0.8 mM[a]

OM	K_{eq} (M^{-1})	polymer M_w (0.8 mM)	theoretical M_w
1	9.4×10^8	340 000	11 000 000
2	3.5×10^7	210 000	2 200 000
3	8.1×10^6	180 000	1 100 000
4	2.8×10^6	78 000	680 000
5	1.3×10^6	76 000	470 000

[a] Theoretical weight-average molecular weights were calculated from the theoretical number-average molecular weight (based on DP from eq 2) and the theoretical polydispersity index (PDI = 2 − (1/DP)).

of the polymers measured from light scattering studies.[66] For reversible polymers, M_w and R_g are changing with the change of concentration. Light scattering measurements show that the conditions for chain overlap are expected to be met at a concentration of 3.8 g/L. At this concentration, an absolute molar mass of 210 kDa and R_g of 28 nm are observed. This value is in excellent agreement with the value extrapolated from the viscosity measurements. Furthermore, the scaling exponent of 3.7 is consistent with theoretical expectation[67] and previous observations for reversible systems.[18]

Thermodynamic Dependence. Reversible polymerization is a dynamic equilibrium process, in which the resulting polymers will finally reach their thermodynamically favored states. The thermodynamic association constant derived from melting experiments is therefore a critical factor to determine the molecular weights. As shown in Table 3, the average molecular weights of 0.8 mM solutions of OM's **1**−**5** increase with association constants *K*. Quantitatively, however, lower-than-expected molecular weights are observed in all OM's studied (Table 3). For example, the measured weight-average molecular weights from OM **2** or **4** are a factor of 10 lower while that from OM **1** is a factor of 30 lower than expected based on eq 2. Furthermore, the observed M_w scales as $K^{0.3}$ instead of the expected value of $K^{0.5}$.

One possible explanation for low molecular weights is the presence of chain-terminating impurities such as failure sequences from the synthesis. We rule out this explanation for two reasons. First, our OM's are carefully purified by HPLC, and subsequent HPLC analysis of the OM's against failure sequence standards shows no impurities. (The detection limit for the HPLC analysis is far lower than the concentrations necessary to explain the differences in molecular weight.) Second, the relative concentration of chain terminators to OM would be independent of total concentration, and so the observed molecular weight would not change with concentration. Because the concentration dependency of the molecular weight agrees well with theoretical expectations (see above), the presence of chain-terminating species is not determining molecular weight.

A second explanation is the presence of smaller, cyclic structures that are more stable than the linear versions for which eqs 1 and 2 were derived. As discussed below, cycle stabilities contribute to the structure of RP's from **4** and **5**, but two pieces of evidence suggest that their presence is only somewhat important for OM's **1**−**3**. First, the viscosity scaling relationships as a function of concentration and MW agree well with theory for

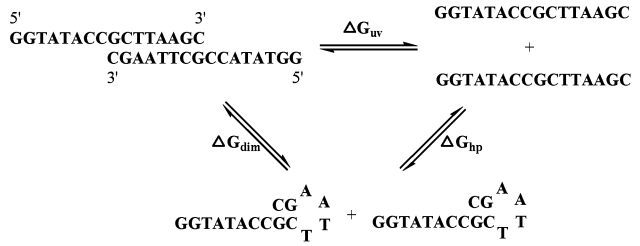

Figure 6. Schematic of energy contributions to thermal melting due to the hairpin formation. ΔG_{dim}, ΔG_{hp}, and ΔG_{uv} are the free energy of dimerization, hairpin formation, and that measured and extrapolated from UV thermal melting, respectively.

rodlike polymers, but they disagree with theory for circular species. Second, enzymatic ligation and digestion of linear polymers formed from 5′-phosphated OM **2** reveals the presence of ∼10% of cyclic structures,[52] an observation that is consistent with expectations for RP's of the observed molecular weights.[68]

We attribute the discrepancy to the formation of moderately stable hairpins that do not contribute to the UV melting studies (as shown in Figure 6). It has been reported that DNA fragments such as d(GCGAAAGC) or d(GCGAAGC) formed stable mini-hairpins with only two G−C base pairs (at room temperature, $\Delta G_{hp} = -4.3$ kcal/mol for the latter, and the stability of the mini-hairpin from the former is even higher although no direct ΔG_{hp} is available so far).[69−72] Similar sequence variants such as d(GCTTAAGC) in **2** or **4**, although perhaps less stable, need only to stabilize the free OM by 1.4 kcal/mol each to account for the difference between the apparent ΔG_{dim} and the measured, relatively high ΔG_{uv}.[69,72] Such weak hairpins might not contribute to ΔG_{uv} (typically measured between 35 and 50 °C) while still factoring into the thermodynamics at room temperature. This modest contribution, in line with those observed in similar structures, would lower the operative association constant *K* by around 2 orders of magnitude. Correspondingly, the expected M_w's would be lowered by 1 order of magnitude, which is consistent with the observed values. A similar contribution of ∼2 kcal/mol due to hairpin formation in OM **1** (d(GCCTAAGC)) would account for the observed 30 times reduction in molecular weight. Similarly, differential hairpin stability would explain the unexpected dependence of M_w on *K*. This explanation was further supported by the fact that, at high temperatures such as 50 °C, the experimental M_w (56 kDa in Figure 7) was reasonably close to the theoretical value of 62 kDa. At elevated temperatures, these weakly stable hairpins are not expected to play a significant thermodynamic role.

Unlike covalent polymers, the molecular weight of RP's might also change with temperature through *K* in eq 2. The reversible association constant between OM's has a strong negative temperature dependence, as determined from variable-concentration UV melting experiments. When the temperature of a 2.5 mM solution of OM **2** is varied from 20 to 50 °C, the molecular weight determined by MALS drops as expected. When plotted against $K(T)$ from the melting studies in Figure 7, the M_w of OM **2** is seen to scale with $K^{0.5}$, consistent with approximately the square-root dependence expected from eq 2.

Conformational Effects. Duplex DNA is a rigid polymer, even with the "nicks" that accompany the reversible analogues described here.[73] We expected that

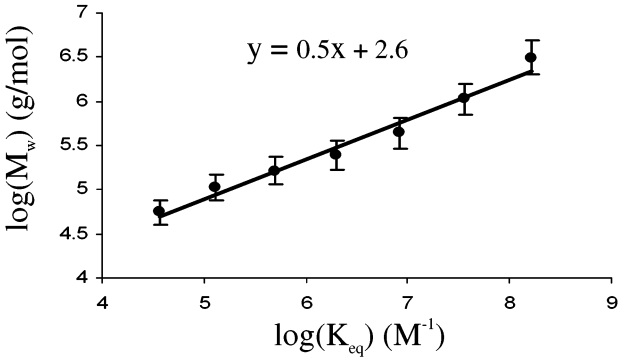

Figure 7. Thermodynamic dependence of the weight-average molecular weights of OM **2** solution (concentration was 2.50 mM and temperatures were varied from 20 to 50 °C). Error bars indicate the uncertainty in M_w as determined from the best fit to the Debye plots (ASTRA software, Wyatt).

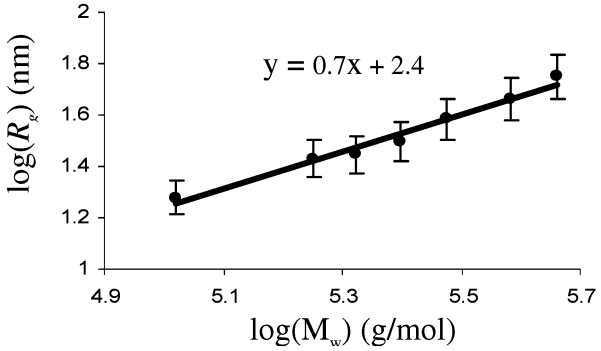

Figure 8. Relationship of the radius of gyration and the weight-average molecular weight of OM **2** (concentrations ranging from 0.16 to 2.30 mM). Error bars indicate the uncertainty in R_g as determined from the best fit to the Debye plots (ASTRA software, Wyatt).

changing the spacer, therefore, would have a dramatic influence on the conformational flexibility of the polymer. For OM **2**, in which there is no spacer, the shape was characterized by measuring R_g at different concentrations (and therefore different molecular weights). The radii of gyration of the resulting truncated polymers were measured by MALS, and the results are plotted against RP molecular weights in Figure 8. The R_g scales as $M_w^{0.7}$. The scaling exponent in this relationship is expected to be equal to $(a + 1)/3$, where a is the Mark−Houwink exponent derived from viscosity relationships.[74] We have previously measured $a = 1.2 \pm 0.1$ for similar systems,[52] and the agreement between the two independent measurements is excellent. These scaling relationships indicate rodlike behavior from the OM-based RP's, consistent with the expected duplex DNA structure. Additional data supporting the expected structure comes from quasi-elastic light scattering (QELS), which provides the hydrodynamic radius R_h to complement measurements of R_g from MALS. The ratio $R_g/R_h = 2.5$ for OM **2** across a M_w range of 100−500 kDa, and that value is indicative of a rodlike polymer.[75,76]

The picture is quite different for OM **4** or OM **5**, which possess a flexible hexaethylene glycol (EG_6) or $(CH_2)_3$ spacer between rigid 8-mer duplexes in their polymerized state. A dramatic difference between **4** and **2** became evident in our initial light scattering characterizations. A 3.0 mM solution of **4** had an initial RP molecular weight of 85 kDa as determined by MALS. This M_w was considerably lower than expected from the empirical and measured association constants of the duplexes. Over the course of 50 h, however, the light scattering signal gradually increased until a final RP molecular weight of 118 kDa was obtained. The time scale for equilibration of OM **4** is 2−3 orders of magnitude slower than that of OM **2**!

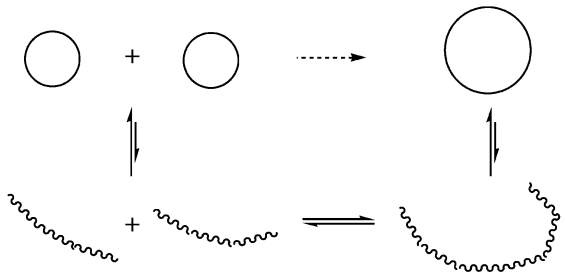

Figure 9. Schematic of the formation of larger cycles from small cyclic RP's. Growth requires two small cyclic RP's to open into two small linear RP's. The time scale for association into longer, linear RP's is long because the equilibrium concentration of small linear RP's is low (a few percent of total RP's). Once formed, the longer linear structure can cyclize to the final thermodynamically favored state.

We interpret this result to reflect the presence of a high number of cyclic RP's in the OM **4** solution. RP extension requires the joining of free ends of two separate RP chains. If a high fraction of RP's exists in cyclic structures, then the concentration of free chain ends is very small. To explain the observed rate reduction, only a few percent of RP's based on OM **4** must exist as linear polymers (Figure 9).

Because average M_w's were lower for **4** or **5** than for **2**, MALS R_g data could be obtained only at a limited number of higher concentrations. This limitation precluded R_g vs M_w analyses similar to those described above. Chain termination experiments coupled to viscosity measurements were more productive, however. When chain terminator **6** was added to a 1.1 mM solution of **4** or **5** in the same manner as described for **2**, above, markedly different results were obtained. In the case of **4** + **6**, the observed viscosity scales with the expected MW of truncated, linear polymers as $M_w^{0.1}$, while in the case of **5** + **6**, it scales as $M_w^{0.3}$. Both are far below the value of 1.1 for rigid rod **2** or even 0.8 expected of random coil polymers. This result provides confirmation that neither OM **4** nor **5** is forming a preponderance of linear RP's and that cyclization probability tends to increase with the longer, flexible spacers.

The cyclization of **4** or **5** is atypical of pure oligonucleotides. The cyclization probabilities of double-stranded DNA have been studied extensively[77−83] and are generally quantified in terms of the effective concentration of one end of a linear DNA strand relative to the other. This "J value" is close to zero for linear, dsDNA of fewer than ∼150 base pairs,[78] and it is fairly insensitive to common structural perturbations such as DNA nicks.[84] Maximum J values are $\sim 10^{-7}$ M,[78,79] meaning that association constants in excess of 10^7 M^{-1} are necessary in order to observe appreciable cyclizations. The cyclic RP's formed from **4** or **5** have 60−120 bp,[85] far fewer than conventional double-stranded DNA or RP's formed from monomers similar to **1**−**3**. Also, the real association constant for OM **4** or **5** is $\sim 10^5$, and so the apparent strong prevalence of cyclic RP's points to a J that is at least 2 orders of magnitude higher than the maximum values observed at DNA lengths of ∼150−300 bp, which are traditionally "ideal" lengths for cyclizations. These

differences signify a dramatic change in the conformational freedom of OM **4** and **5** vs wholly nucleotide OM's **1**−**3**.

Conclusion

Oligonucleotide-based monomers are shown to constitute a useful chemical system for the study of reversible polymerization. Viscometry, size exclusion chromatography, and static and dynamic multiangle light scattering provide quantitative insights into the equilibrium and dynamic properties of the polymeric structures. Slight changes in the primary base sequence result in varied thermodynamics of association that are reflected in the molecular weights of resulting polymeric assemblies. When the monomers comprise only nucleotides, the polymers resemble double-stranded DNA, and the only significant differences in structure are due to the degree of polymerization. Concentration and temperature dependencies further reflect the expected equilibrium behavior of main-chain reversible polymers, although hairpin formation makes unexpected contributions to the stability of free monomers. Incorporation of synthetic spacers between the oligonucleotides within a monomer can have a substantial influence on the conformational properties of the monomer and resulting assemblies, as evidenced here by dramatic increases in cyclization probabilities and time scales for equilibration. In all cases, the structure and behavior of the polymers can be attributed to controlled features of the molecular, monomeric constituents. Thus, DNA-based reversible polymers represent a modular and well-behaved chemical system for the study of fundamental reversible polymer processes in complex environments that are poorly understood.

Acknowledgment. This work was supported by the Donors of the Petroleum Research Fund of the American Chemical Society and Duke University. Partial support was provided by the North Carolina Biotechnology Center and Research Corp. S.L.C. gratefully acknowledges a DuPont Young Professor Award and a Camille and Henry Dreyfus New Faculty Award.

Supporting Information Available: Figures of representative melting curve of OM **2**, thermodynamic parameters of OM **1**−**5**, representative light scattering data, and DNA purity; derivation of DP equation (eq 1 in text). This material is available free of charge via the Internet at http://pubs.acs.org.

References and Notes

(1) Brunsveld, L.; Folmer, B. J. B.; Meijer, E. W.; Sijbesma, R. P. *Chem. Rev.* **2001**, *101*, 4071−4097.
(2) Sijbesma, R. P.; Meijer, E. W. *Chem. Commun.* **2003**, 5−16.
(3) Schmuck, C.; Wienand, W. *Angew. Chem., Int. Ed.* **2001**, *40*, 4363−4369.
(4) ten Cate, A. T.; Sijbesma, R. P. *Macromol. Rapid Commun.* **2002**, *23*, 1094−1112.
(5) Corbin, P. S.; Zimmerman, S. C. In *Supramolecular Polymers*; Ciferri, A., Ed.; Marcel Dekker: New York, 2000; Vol. 1, pp 147−176.
(6) van der Gucht, J.; Bessling, N. A. M.; Stuart, M. A. C. *J. Am. Chem. Soc.* **2002**, *124*, 6202−6205.
(7) Lehn, J.-M. *Macromol. Chem. Macromol. Symp.* **1993**, *69*, 1.
(8) Sijbesma, R. P.; Beijer, F. H.; Brunsveld, L.; Folmer, B. J. B.; Hirschberg, J. H. K. K.; Lange, R. F. M.; Lowe, J. K. L.; Meijer, E. W. *Science (Washington, D.C.)* **1997**, *278*, 1601−1604.
(9) Castellano, R. K.; Rudkevich, D. M.; Rebek, J., Jr. *Proc. Natl. Acad. Sci. U.S.A.* **1997**, *94*, 7132−7137.
(10) Zimmerman, N.; Moore, J. S.; Zimmerman, S. C. *Chem. Ind.* **1998**, 604−610.
(11) Alexander, C.; Jariwala, C. P.; Lee, C. M.; Griffin, A. C. *Polym. Prepr. (Am. Chem. Soc., Div. Polym. Chem.)* **1993**, *34*, 168−169.
(12) Michelsen, U.; Hunter, C. A. *Angew. Chem., Int. Ed.* **2000**, *39*, 764−767.
(13) Whitesides, G. M.; Mathias, J. P.; Seto, C. T. *Science* **1991**, *254*, 1312−1319.
(14) Castellano, R. K.; Nuckolls, C.; Eichhorn, S. H.; Wood, M. R.; Lovinger, A. J.; Rebek, J., Jr. *Angew. Chem., Int. Ed.* **1999**, *38*, 2603−2606.
(15) Hirschberg, J. H. K. K.; Ramzi, A.; Sijbesma, R. P.; Meijer, E. W. *Macromolecules* **2003**, *36*, 1429−1432.
(16) Keizer, H. M.; Sijbesma, R. P.; Jansen, J. F. G. A.; Pasternack, G.; Meijer, E. W. *Macromolecules* **2003**, *36*, 5602−5606.
(17) Canty, A. J.; Patel, J.; Skelton, B. W.; While, A. H. *J. Organomet. Chem.* **2000**, *599*, 195−199.
(18) Castellano, R. K.; Clark, R.; Craig, S. L.; Nuckolls, C.; Rebek, J., Jr. *Proc. Natl. Acad. Sci. U.S.A.* **2000**, *97*, 12418−12421.
(19) Hilger, C.; Stadler, R. *Makromol. Chem.* **1991**, *192*, 805−817.
(20) Dankers, P. Y. W.; van Beek, D. J. M.; ten Cate, A. T.; Sijbesma, R. P.; Meijer, E. W. *Polym. Mater. Sci. Eng.* **2003**, *88*, 52−53.
(21) ten Cate, A. T.; van Beek, D. J. M.; Spiering, A. J. H.; Dankers, P. Y. W.; Sijbesma, R. P.; Meijer, E. W. *Polym. Prepr. (Am. Chem. Soc., Div. Polym. Chem.)* **2003**, *44*, 618−619.
(22) Sijbesma, R. P.; Folmer, B. J. B.; Meijer, E. W. *Polym. Prepr. (Am. Chem. Soc., Div. Polym. Chem.)* **2002**, *43*, 375−376.
(23) Bosman, A. W.; Folmer, B. J. B.; Hirschberg, J. H. K. K.; Keizer, H. M.; Sijbesma, R. P.; Meijer, E. W. *Polym. Prepr. (Am. Chem. Soc., Div. Polym. Chem.)* **2002**, *43*, 322.
(24) Knapp, R.; Schott, A.; Rehahn, M. *Macromolecules* **1996**, *29*, 478−480.
(25) Meier, M. A. R.; Schubert, U. S. *Polym. Mater. Sci. Eng.* **2003**, *88*, 443−444.
(26) Hofmeier, H.; Gohy, J.-F.; Schubert, U. S. *Polym. Mater. Sci. Eng.* **2003**, *88*, 193−194.
(27) Hofmeier, H.; El-Ghayoury, A.; Schubert, U. S. *Polym. Prepr. (Am. Chem. Soc., Div. Polym. Chem.)* **2003**, *44*, 711−712.
(28) Hofmeier, H.; Schmatloch, S.; Schubert, U. S. *Polym. Prepr. (Am. Chem. Soc., Div. Polym. Chem.)* **2003**, *44*, 709−710.
(29) Schmatloch, S.; Gonzalez, M. F.; Schubert, U. S. *Macromol. Rapid Commun.* **2002**, *23*, 957−961.
(30) Gohy, J.-F.; Lohmeijer, B. G. G.; Varshney, S. K.; Decamps, B.; Leroy, E.; Boileau, S.; Schubert, U. S. *Macromolecules* **2002**, *35*, 9748−9755.
(31) Lohmeijer, B. G. G.; Schubert, U. S. *Angew. Chem., Int. Ed.* **2002**, *41*, 3825−3829.
(32) Schubert, U. S.; Schmatloch, S.; Precup, A. A. *Des. Monomers Polym.* **2002**, *5*, 211−221.
(33) Schubert, U. S.; Eschbaumer, C. *Angew. Chem., Int. Ed.* **2002**, *41*, 2892−2926.
(34) Gohy, J.-F.; Lohmeijer, B. G. G.; Varshney, S. K.; Schubert, U. S. *Macromolecules* **2002**, *35*, 7427−7435.
(35) Rowan, S. J.; Beck, J. B.; Ineman, J. M. *Polym. Prepr. (Am. Chem. Soc., Div. Polym. Chem.)* **2003**, *44*, 691−692.
(36) Rowan, S. J.; Suwanmala, P.; Sivakova, S. *J. Polym. Sci., Part A: Polym. Chem.* **2003**, *41*, 3589−3596.
(37) Harada, A.; Kawaguchi, Y.; Hoshino, T. *J. Inclusion Phenom.* **2001**, *41*, 115−121.
(38) Berl, V.; Schmutz, M.; Krische, M. J.; Khoury, R. G.; Lehn, J.-M. *Chem.—Eur. J.* **2002**, *8*, 1227−1244.
(39) Harada, A. *Kagaku Kyoiku* **2002**, *50*, 86−88.
(40) Fromm, K. M. *Chem.—Eur. J.* **2001**, *7*, 2236−2244.
(41) Boileau, S.; Bouteiller, L.; Laupretre, F.; Lortie, F. *New J. Chem.* **2000**, *24*, 845−848.
(42) Harada, A. *Kagaku Kogyo (Osaka)* **2000**, *74*, 470−476.
(43) Moore, J. S. *Curr. Opin. Colloid Interface Sci.* **1999**, *4*, 108−116.
(44) Hirschberg, J. H. K. K.; Beijer, F. H.; van Aert, H. A.; Magusin, P. C. M. M.; Sijbesma, R. P.; Meijer, E. W. *Macromolecules* **1999**, *32*, 2696−2705.
(45) Gibson, H. W.; Yamaguchi, N.; Jones, J. W. *J. Am. Chem. Soc.* **2003**, *125*, 3522−3533.
(46) Cooke, G.; Rotello, V. M. *Chem. Soc. Rev.* **2002**, *31*, 275−286.
(47) Stubbs, L. P.; Weck, M. *Chem.—Eur. J.* **2003**, *9*, 992−999.
(48) Kilian, L.; Yamauchi, K.; Sinani, V. A.; Hudelson, C. L.; Long, T. E. *Polym. Prepr. (Am. Chem. Soc., Div. Polym. Chem.)* **2002**, *43*, 916−917.

(49) Elkins, C. L.; Yamauchi, K.; Long, T. E. *Polym. Prepr. (Am. Chem. Soc., Div. Polym. Chem.)* **2003**, *44*, 576−577.
(50) Folmer, B. J. B.; Sijbesma, R. P.; Meijer, E. W. *Polym. Mater. Sci. Eng.* **1999**, *80*, 20−21.
(51) Brunsveld, L.; Folmer, B. J. B.; Meijer, E. W. *MRS Bull.* **2000**, *25*, 49−53.
(52) Fogleman, E. A.; Yount, W. C.; Xu, J.; Craig, S. L. *Angew. Chem., Int. Ed.* **2002**, *41*, 4026−4028.
(53) Seeman, N. C. *Angew. Chem., Int. Ed.* **1998**, *37*, 3220−3238.
(54) Guckian, K. M.; Schweitzer, B. A.; Ren, R. X.-F.; Sheils, C. J.; Tahmassebi, D. C.; Kool, E. T. *J. Am. Chem. Soc.* **2000**, *122*, 2213−2222.
(55) Bommarito, S.; Peyret, N.; SantaLucia, J., Jr. *Nucleic Acids Res.* **2000**, *28*, 1929−1934.
(56) (a) Breslauer, K. J.; Frank, R.; Blocker, H.; Marky, L. A. *Proc. Natl. Acad. Sci. U.S.A.* **1986**, *83*, 3746. (b) Plum, G. E.; Breslauer, K. J.; Roberts, R. W. *Compr. Nat. Prod. Chem.* **1999**, *7*, 15−53.
(57) Nicolai, T.; Mandel, M. *Macromolecules* **1989**, *22*, 438−444.
(58) For other examples of light scattering in the study of reversible polymerization, see: (a) Lomakin, A.; Benedek, G. B.; Castellano, R. K.; Nuckolls, C.; Rebek, J., Jr. *Trends Opt. Photonics* **2002**, *47*, 27−29. (b) van der Gucht, J.; Besseling, N. A. M.; Knoben, W.; Bouteiller, L.; Cohen Stuart, M. A. *Phys. Rev. E* **2003**, *67*, 051106/1-051106/10.
(59) Xu, J.; Craig, S. L., unpublished results.
(60) Wissenburg, P.; Odijk, T.; Cirkel, P.; Mandel, M. *Macromolecules* **1995**, *28*, 2315−2328.
(61) Stigter, D.; Dill, K. A. *J. Phys. Chem.* **1993**, *97*, 12995−12997.
(62) Folmer, B. J. B.; Cavini, E.; Sijbesma, R. P.; Meijer, E. W. *Chem. Commun.* **1998**, 1847−1848.
(63) Wu, A.; Isaacs, L. *J. Am. Chem. Soc.* **2003**, *125*, 4831−4835.
(64) Ciferri, A. *Macromol. Rapid Commun.* **2002**, *23*, 511−529.
(65) We earlier reported an average slope of 3.3 for OM **2** (see *Angew. Chem., Int. Ed.* **2002**, *41*, 4026−4028). Further measurements and closer inspection reveal the transition from dilute to semidilute regimes.
(66) Pan, C.; Maurer, W.; Liu, Z.; Lodge, T. P. *Macromolecules* **1995**, *28*, 1643−1653.
(67) Cates, M. E. *Macromolecules* **1987**, *20*, 2289.
(68) The percentage of cyclic components can be estimated as the product of the effective association constant and the *J* value. In this case, the effective association constant is on the order of 10^6, while the *J* value on the order of 10^{-7}, the percentage of cyclic components therefore can be estimated roughly as 10%.
(69) Hirao, I.; Nishimura, Y.; Tagawa, Y.; Watanabe, K.; Miura, K. *Nucleic Acids Res.* **1992**, *20*, 3891−3896.
(70) Yoshizawa, S.; Kawai, G.; Nishimura, Y.; Kakinuma, T.; Matsumoto, N.; Ishido, Y.; Miura, K.; Watanabe, K.; Hirao, I. *Nucleic Acids Symp. Ser.* **1994**, *31*, 293−294.
(71) Yoshizawa, S.; Ueda, T.; Ishido, Y.; Miura, K.; Watanabe, K.; Hirao, I. *Nucleic Acids Res.* **1994**, *22*, 2217−2221.
(72) Yoshizawa, S.; Kawai, G.; Watanabe, K.; Miura, K.; Hirao, I. *Biochemistry* **1997**, *36*, 4761−4767.
(73) Mills, J. B.; Cooper, J. P.; Hagerman, P. J. *Biochemistry* **1994**, *33*, 1797−1803.
(74) Varadaiah, V. V.; Rao, V. S. R. *J. Polym. Sci.* **1959**, *36*, 558−559.
(75) Burchard, W.; Schmidt, M.; Stockmayer, W. H. *Macromolecules* **1980**, *13*, 1265−1272.
(76) Schmidt, M. *Macromolecules* **1984**, *17*, 553−560.
(77) Jacobson, H.; Stockmayer, W. H. *J. Chem. Phys.* **1950**, *18*, 1600−1606.
(78) Shimada, J.; Yamakawa, H. *Macromolecules* **1984**, *17*, 689−698.
(79) Shore, D.; Baldwin, R. *J. Mol. Biol.* **1983**, *170*, 957−981.
(80) Crothers, D.; Drak, J.; Kahn, J.; Levene, S. *Methods Enzymol.* **1992**, *212*, 3−29.
(81) Shore, D.; Langowski, J.; Baldwin, R. *Proc. Natl. Acad. Sci. U.S.A.* **1981**, *78*, 4833−4837.
(82) Yamakawa, H.; Stockmayer, W. H. *J. Chem. Phys.* **1972**, *57*, 2843.
(83) Dlakic, M.; Harrington, R. *J. Biol. Chem.* **1995**, *270*, 29945−29952.
(84) Zhang, Y.; Crothers, D. M. *Proc. Natl. Acad. Sci. U.S.A.* **2003**, *100*, 3161−3166.
(85) The value obtained by light scattering reflects the weight-average MW and corresponds to a polymer with ∼120 bp. If the polydispersity index is close to the theoretical value of 2 expected for linear RP's, then the number average of base pairs per chain is ∼60 bp.

MA035546V